Recueil De Mécanique
El Wancharissi University
of Tissemsilt

Research Paper DOI : 10.5281/zenodo.5918550 Open access

Static study of functionally graded material (FGM) sandwich plates using a new hyperbolic theory

Soumia BENGUEDIAB[a],Fatima Zohra KETTAF[b], Mohamed BENGUEDIAB[c,*], Abdelouhed TOUNSI[d]

[a] *Department of Civil Engineering and Hydraulic, University Dr Moulay Tahar of Saida, Algeria*

[b]*Department of Mechanical Engineering, Faculty of Mechanical Engineering University of Science and Technology Mohamed Boudiaf Oran, Algeria.*

[c]*Department of Mechanical Engineering, University Djillali Liabes of Sidi Bel Abbes, Algeria*

[d]*Department of Civil Engineering, University Djillali Liabes of Sidi Bel Abbes, Algeria*

ARTICLE INFO

Article history :

Received 26 August 21

Accepted 08 January 22

Keywords:

FGM plate ; Hyperbolic theory ;Refined theory ;Navier solution.

ABSTRACT

A new refined hyperbolic theory taking into account the transverse shear effect is proposed to analyze the static behavior of thick plates in functionally graduated materials (FGM). The proposed model uses a new displacement field using only four unknowns determining the equilibrium equations, using the Hamilton principle. This theory contains only four variables unlike other plate theories. The nullity of transverse shear stresses at the upper and lower surfaces of the plate is satisfied in this model. These material properties of the FGM plate vary according to a distribution of the power law in terms of volume fraction of the constituents; one can conclude that this theory is effective and simple for the analysis of the static response of the FGM plates.

1 Introduction

Functionally graded material (FGM) is a special combination of ceramics and metals designed to endure high thermal environment and to provide stiffness to the host structure. Volume fraction and material properties of such materials are continuous and smooth along the direction under consideration. Abrupt change in the elastic properties and thermal coefficients in the composite laminates results in high interlaminar stresses leading to delamination. FGM is a better alternative to the composite laminates because of a gradual change in their elastic properties, particularly along the thickness direction. Koizumi [1] proposed the concept of FGM, which was initiated by material scientists in the Sendai area of Japan [2]. FGM sandwich structures in the various fields of aerospace, marine and civil construction have seen increasing use given the very high strength / weight ratio. Understanding the static and vibrational behavior of these

* *Corresponding author. Tel.: +213 777741710.*
E-mail address: benguediabm@gmail.com

sandwich structures becomes an important task. Some researchers have studied the bending, buckling and free vibrations of the FGM plates using plate theories. The classical plate theory (CPT) is the simplest of the deformation and it supposes a plane normal to the median plane before folding remains flat and normal after folding. He neglects the effect of all transverse constraints and is less precise. Therefore, it gives accurate results for thin plates only. Feldman and Aboudi [3], Javaheri and Islami [4] then Chi and Chung [5] have obtained static response of FGPs using CPT. The disadvantage of CPT was overcome by first-order shear deformation theory (FSDT) proposed by Reissner [6] and Mindlin [7] which considers the effect of transverse shear strain. This theory does not satisfy boundary conditions without stress on the plate surfaces and requires an arbitrary shear correction factor. The FSDT theory to study the mechanical behavior of the plates has been used by many authors [8-11]. The first theories on shear deformation have been proposed by Reissner [12] and Mindlin [7]. Mindlin's theory assumes that displacement varies linearly over the thickness of the plate. This theory requires a correction factor to satisfy the conditions of free transverse shear stress on the upper and lower surfaces of the plate. Different models have been developed to analyze the static and dynamic behavior of these structures in FGM. Higher order shear deformation (HSDT) theories have been proposed to eliminate the use of the shear correction factor to overcome the limitations of FSDT. These theories use higher-order terms in Taylors' development of displacements in the FSDT. These theories are based on the variation of displacement across the thickness of the plate using Reddy polynomial functions [13] or non-polynomial functions Touratier [14], the hyperbolic theory of Soldatos [15] or an exponential theory developed by Karama et al. [16].

Zenkour [17] did a complete study to analyze the static response of FGM sandwich plates subjected to a sinusoidal load using different plate theories. The free vibration of FGM sandwich rectangular plates with simply supported and clamped edges using the Ritz method has been investigated by Li et al. [18]. Subsequently Zenkour and Alghamdi [19] developed a unified shear deformable plate and performed thermoelastic bending analysis of FGM sandwich plate.

In recent years, many researchers have studied the effect of stretching thickness on FGM structures [20-27]. A new hyperbolic shear deformation theory for bending and free vibration analysis of isotropic, functionally graded, sandwich and laminated composite plates has been proposed by Mahi et al. [28] and Merdaci [29].

In the present study, the development of a new refined hyperbolic theory taking into account the transverse shear effect is proposed to analyze the static behavior of thick plates in functionally graduated materials (FGM). Three common types of FGM sandwich plates namely, isotropic FG plates (Type A) ,sandwich plates with FG core (Type B) and sandwich plates with FG faces (Type C) are considered.

2 Theoretical Formulation

2.1 Geometrical configuration

A rectangular plate made FGMs whose geometry and dimensions (length a, width b and uniform thickness h) are shown in figure 1 a transverse mechanical load at the top area and a compressive load in the mid-plane are applied subject to plate. Three types of FG plates are considered in this study

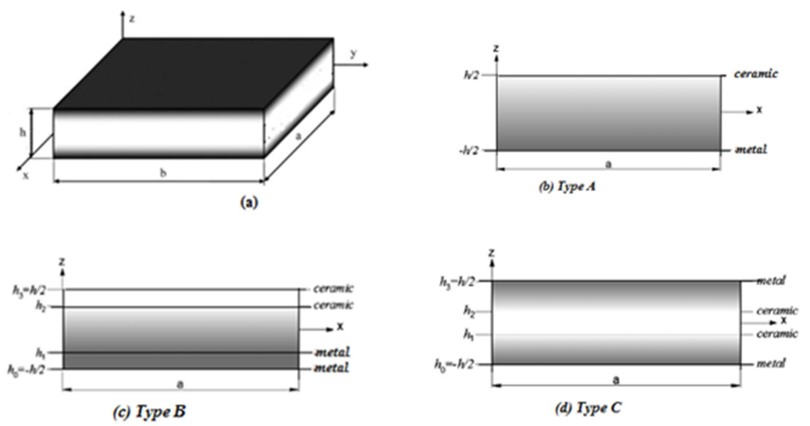

Fig. 1 – Geometry of rectangular FGM plates [30]

Type A: plate is made of metal on its bottom surface and ceramic on the top surface (Fig. 1b) .Ceramic has a volume fraction Vc varying as following:

$$V_c(z) = \left(\frac{2z+h}{2h}\right)^p \quad (1)$$

Type B: sandwich plates with FG core (Fig. 1c): this type of core is made on the underside of metal and on the upper side of ceramic. The vertical positions of the bottom and top surfaces, and two interfaces between the layers are designated By $h_0 = -\frac{h}{2}$, h_1, h_2, $h_3 = \frac{h}{2}$ respectively. h_1, h_2 vary according the thickness ratio of layers. The volume fraction functions of ceramic phase V_C^j defined by:

$$V^1(z) = 0\ for\ z \in [\![h_0, h_1]\!]$$

$$V^2(z) = (\frac{z-h}{h_2\_h_1})^p\ for\ z \in [\![h_1, h_2]\!] \quad (2)$$

$$V^3(z) = 1\ for\ z \in [\![h_2, h_3]\!]$$

Type C: it is sandwich plates with faces FG: The faces of these types are gradually made up of a metal towards a ceramic. Isotropic ceramics constitute the core.The volume fraction functions of ceramic phase V_C^j defined by:

$$V^1(z) = (\frac{z-h_0}{h_1\_h_0})^p\ for\ z \in [\![h_0, h_1]\!]$$

$$V^2(z) = 1\ ,for\ z \in [\![h_1, h_2]\!] \quad (3)$$

$$V^3(z) = (\frac{z-h_2}{h_2\_h_3})^p\ ,for\ z \in [\![h_2, h_3]\!]$$

The variation of ceramic material through the plate thickness for (1-2-1) sandwich plate of Type B and sandwich plate of Type C are represented respectively in figures 2a and 2b

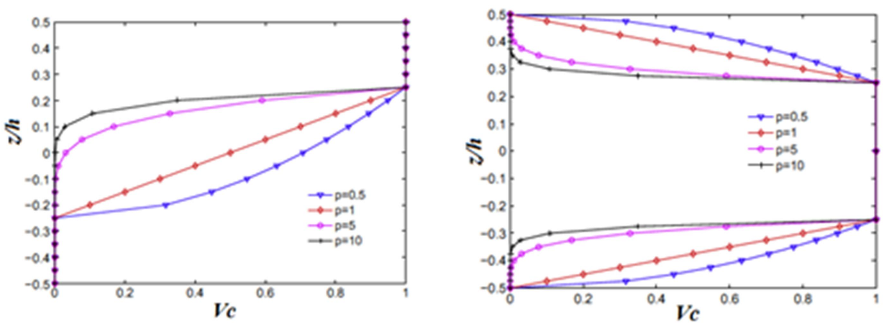

(a) Type B **(b) Type C**

Fig. 2– Sandwich plates for several power-law index p

3 Kinematics and Strains

In this study, further simplifying supposition are made to the conventional HSDT so that the number of unknowns is reduced. The displacement field of the conventional HSDT is given by:

$$u(x.y.z) = u_0(x,y) - z\frac{\partial w_0}{\partial x} + f(z)\theta(x,y)$$

$$v(x.y.z) = u_0(x.y) - z\frac{\partial w_0}{\partial y} + f(z)\theta(x,y) \quad (4)$$

$$w(x.y.z) = w_0(x.y)$$

The function f(z) is given by:

$$f(z) = \sinh(z) - \frac{4}{3}z^3\cosh(\frac{1}{2}) \tag{5}$$

Where u, v, w, θ are displacements of the medium fiber of plate and f(z) indicates the function of the shape determining the distribution of transverse shear deformations and stresses in the direction of thickness. Equations (4) can be written in compacted form:

$$\varepsilon = \varepsilon^{(1)} + z\varepsilon^{(2)} + f\varepsilon^{(3)} \text{ and } \gamma = g\gamma^{(0)} \tag{6}$$

Where g=df/dz, $\varepsilon^{(0)}$, $\varepsilon^{(1)}$, $\varepsilon^{(2)}$ and $\gamma^{(0)}$ are respectively the deformations of membrane, curvature and transverse deformation. These equations are related to the displacement field of equation (4) as follows:

$$\varepsilon^{(0)} = \begin{Bmatrix} \varepsilon_x^{(0)} \\ \varepsilon_y^{(0)} \\ \gamma_{xy}^{(0)} \end{Bmatrix} = \begin{Bmatrix} \frac{\partial u_0}{\partial x} \\ \frac{\partial v_0}{\partial y} \\ \frac{\partial u_0}{\partial y} + \frac{\partial v_0}{\partial x} \end{Bmatrix} \tag{7a}$$

$$\varepsilon^{(1)} = \begin{Bmatrix} \varepsilon_x^{(1)} \\ \varepsilon_y^{(1)} \\ \gamma_{xy}^{1} \end{Bmatrix} = \begin{Bmatrix} -\frac{\partial^2 w_0}{\partial^2 x} \\ -\frac{\partial^2 w_0}{\partial^2 y} \\ -\frac{\partial^2 w_0}{\partial x \partial y} \end{Bmatrix} \tag{7b}$$

$$\varepsilon^{(2)} = \begin{Bmatrix} \varepsilon_x^{(1)} \\ \varepsilon_y^{(1)} \\ \gamma_{xy}^{(1)} \end{Bmatrix} = \begin{Bmatrix} \frac{\partial \theta_x}{\partial x} \\ \frac{\partial \theta_y}{\partial y} \\ \frac{\partial u_0}{\partial y} + \frac{\partial v_0}{\partial x} \end{Bmatrix} \tag{7c}$$

$$\gamma^{(0)} = \begin{Bmatrix} \gamma_{yz}^{(0)} \\ \gamma_x^{(0)} \end{Bmatrix} = \begin{Bmatrix} \theta_x \\ \theta_y \end{Bmatrix} \tag{7d}$$

4 Kinematics and Strains

Hamilton's principle is used herein to derive the equations of motion. The principle can be stated in analytical form as:

$$\int_0^T (\partial U + \partial V)dt = 0 \tag{8}$$

Where ∂U the variations of strain energy, ∂V the variations of work done of the plate. The variations of strain energy are given by:

$$\delta u = \int_A \int_{-\frac{h}{2}}^{\frac{h}{2}} (\sigma_{xx}\delta\varepsilon_{xx} + \sigma_{yy}\delta\varepsilon_{yy} + \sigma_{xy}\delta\gamma_{xy} + \sigma_{xz}\delta\gamma_{xz} + \sigma_{yz}\delta\gamma_{yz})dAdZ = \int_A [N_{xx}\frac{\partial \delta u_0}{\partial x} - M_{xx}\frac{\partial^2 \delta W_0}{\partial^2 x} + R_{xx}\frac{\partial \delta\theta_x}{\partial x} + N_{yy}\frac{\partial \delta v_0}{\partial y} - M_{yy}\frac{\partial^2 \delta W_0}{\partial^2 y} - R_{yy}\frac{\partial \delta\theta_y}{\partial y} + N_{xy}\left(\frac{\partial \delta u_0}{\partial y} + \frac{\partial \delta v_0}{\partial x}\right) - 2M_{xy}\frac{\partial^2 \delta W_0}{\partial x \partial y} + R_{xy}\left(\frac{\partial \delta\theta_X}{\partial y} + \frac{\partial \delta\theta_y}{\partial x}\right) + Q_x\delta\theta_x + Q_y\delta\theta_y]dA \tag{9}$$

Where N, M, R and Q are the resultants of the constraints defined by:

$$(N_{XX}, N_{yy}, N_{xy}) = \int_{-h/2}^{h/2} (\sigma_{xx}, \sigma_{yy}, \sigma_{xy})d_z \tag{10a}$$

$$(M_{XX}, M_{yy}, M_{xy}) = \int_{-h/2}^{h/2} z(\sigma_{xx}, \sigma_{yy}, \sigma_{xy})d_z \tag{10b}$$

$$(R_{XX}, R_{yy}, R_{xy}) = \int_{-h/2}^{h/2} f(\sigma_{xx}, \sigma_{yy}, \sigma_{xy})d_z \tag{10c}$$

$$(Q_X, Q_y) = \int_{-h/2}^{h/2} g(\sigma_{xz}, \sigma_{yz})d_z \tag{10d}$$

The variation of the work is given by:

$$\delta V = \int_A q\delta w_0 \, dA \tag{11}$$

Substituting equations (9) and (11) in equation (8), integrating into parts and collecting the coefficients δu_0, δv_0, δw_0, and $\delta\theta_0$,we obtain the equations of motion:

$$\delta \mathrm{u}_0 = \frac{\partial \mathrm{Nxx}}{\partial x} + \frac{\partial Nxy}{\partial y} = 0 \tag{12a}$$

$$\delta \vartheta_0 = \frac{\partial \mathrm{Nxy}}{\partial x} + \frac{\partial Nyy}{\partial y} = 0 \tag{12b}$$

$$\delta w_0 \ = \frac{\partial^2 Mxx}{\partial x^2} + 2\frac{\partial^2 Mxy}{\partial x \partial y} + \frac{\partial^2 Myy}{\partial y^2} + \mathrm{q} = 0 \tag{12c}$$

$$\delta\theta_0 = \frac{\partial Rxx}{\partial x} + \frac{\partial Rxy}{\partial y} + \frac{\partial Rxy}{\partial x} + \frac{\partial Ryy}{\partial y} - Q_x - Q_y = 0 \tag{12d}$$

The material properties of the layers of the FGM plate related to the law of force are expressed by:

$$P^{(i)}(z) = (P_C - P_m)V_c^{(j)} + P_m \tag{13}$$

Where Pc and Pm are the Young's modulus (E), Poisson's ratio (ν), mass densities (ρ) of metal and ceramic materials, respectively. For elastic and isotropic FG plates, the constitutive relations can be written as:

$$\begin{Bmatrix} \sigma_{xx} \\ \sigma_{yy} \\ \sigma_{xy} \end{Bmatrix} = \begin{bmatrix} c_{11} & c_{12} & 0 \\ c_{21} & c_{22} & 0 \\ 0 & 0 & c_{66} \end{bmatrix} \begin{Bmatrix} \varepsilon_{xx} \\ \varepsilon_{yy} \\ \gamma_{xy} \end{Bmatrix} \tag{14a}$$

$$\begin{Bmatrix} \sigma_{xz} \\ \sigma_{yz} \end{Bmatrix} = \begin{bmatrix} c_{55} & 0 \\ 0 & c_{44} \end{bmatrix} \begin{Bmatrix} \gamma_{xz} \\ \gamma_{yz} \end{Bmatrix} \tag{14b}$$

Where:

$$c_{11}(z) = c_{22}(z) = \frac{E(z)}{1-\vartheta(z)^2} \ ; \qquad c_{12}(z) = \vartheta(z) c_{11}(z) \tag{15a}$$

$$c_{44}(z) = c_{55}(z) = c_{66}(z) = \frac{E(z)}{2(1+\vartheta(z))} \tag{15b}$$

Substituting Eq. (7b) into Eq. (14a) and the subsequent results into Eqs. (10a), (10b) and (10c), the stress resultants are obtained in terms of strains as following compact form:

$$\begin{Bmatrix} N \\ M \\ R \end{Bmatrix} = \begin{bmatrix} A & B & B^5 \\ B & D & D^5 \\ B^5 & D^5 & H^s \end{bmatrix} \begin{Bmatrix} \varepsilon^{(1)} \\ \varepsilon^{(2)} \\ \varepsilon^{(3)} \end{Bmatrix} \tag{16}$$

Where A, B, D, B^s, D^s, H^s are the stiffnesses of the FGM plate given by:

$$(A, B, D, B^5, D^5, H^5) = \int_{-h/2}^{h/2} (1, z, z^2, f, zf, f^2) c(z) dz \tag{17}$$

The transverse forces can be calculated from the constitutive equations by replacing Eq. (7b) into Eq. (14b and the subsequent results into Eq. (10d). The transverse forces can be written as follows:

$$\begin{Bmatrix} Q_x \\ Q_y \end{Bmatrix} = \begin{bmatrix} A_{55}{}^5 & 0 \\ 0 & A_{44}{}^5 \end{bmatrix} \begin{Bmatrix} \gamma_{xz}^{(0)} \\ \gamma_{yz}^{(0)} \end{Bmatrix} \tag{18}$$

In the compact form Eq. (18) can be reduced as follows:

$$Q = A^s \gamma^0 \tag{19}$$

Where A^5 are the shear stiffnesses of the FGM plate given by:

$$A_{44}{}^5 \ = A_{55}{}^5 \ = \int_{-\frac{h}{2}}^{\frac{h}{2}} g^2(z) c_{44}(z) \ dz = \int_{-\frac{h}{2}}^{\frac{h}{2}} g^2(z) \ c_{55}(z) \ dz \tag{20}$$

Substituting Eq. (16) and Eq. (19) into Eq. (12), the equations of motion can be expressed in terms of displacement (u_0, $\mathrm{v}_0, \delta \mathrm{w}_0$, $\delta\theta_0$) as follows:

$$a_{11}\frac{\partial^2}{\partial x^2}u_0(x,y)-b_{11}\frac{\partial^3}{\partial x^3}w_0(x,y)+b_{11}^S\frac{\partial^2}{\partial x^2}\theta_0(x,y)+a_{12}\frac{\partial^2}{\partial x\,\partial y}v_0(x,y)-b_{12}\frac{\partial^3}{\partial y^2\,\partial x}w_0(x,y)+b_{12}^S\frac{\partial^2}{\partial x\,\partial y}\theta_0(x,y)+a_{66}\frac{\partial^2}{\partial y^2}u_0(x,y)+a_{66}\frac{\partial^2}{\partial y\,\partial x}v_0(x,y)-2a_{11}\frac{\partial^3}{\partial y^2\,\partial x}w_0(x,y)+b_{66}^S\frac{\partial^2}{\partial y^2}\theta_0(x,y)+b_{66}^S\frac{\partial^2}{\partial y\,\partial x}\theta_0(x,y)=0 \tag{21a}$$

$$a_{12}\frac{\partial^2}{\partial x\,\partial y}u_0(x,y)-b_{12}\frac{\partial^3}{\partial y\,\partial x^2}w_0(x,y)+b_{12}^S\frac{\partial^2}{\partial y\,\partial x}\theta_0(x,y)+a_{22}\frac{\partial^2}{\partial y^2}v_0(x,y)-b_{22}\frac{\partial^3}{\partial y^3}w_0(x,y)+b_{22}^S\frac{\partial^2}{\partial y^2}\theta_0(x,y)-+a_{66}\frac{\partial^2}{\partial x\,\partial y}u_0(x,y)+a_{66}\frac{\partial^2}{\partial x^2}v_0(x,y)+2b_{66}\frac{\partial^3}{\partial y\,\partial x^2}w_0(x,y)+b_{66}^S\frac{\partial^3}{\partial y\,\partial x^2}\theta_0(x,y)+b_{66}^S\frac{\partial^2}{\partial y\,\partial x}\theta_0(x,y)=0 \tag{21b}$$

$$b_{11}\frac{\partial^3}{\partial x^3}u_0(x,y)-d_{11}\frac{\partial^4}{\partial y^2\,\partial x^2}w_0(x,y)+d_{11}^S\frac{\partial^3}{\partial x^3}\theta_0(x,y)+b_{12}\frac{\partial^3}{\partial y\,\partial x^2}v_0(x,y)-2d_{12}\frac{\partial^4}{\partial x^2\,\partial y^2}w_0(x,y)+d_{12}^S\frac{\partial^3}{\partial y\,\partial x^2}\theta_0(x,y)+b_{22}\frac{\partial^3}{\partial y^3}v_0(x,y)-d_{22}\frac{\partial^4}{\partial y^4}w_0(x,y)+d_{22}^S\frac{\partial^3}{\partial y^3}\theta_0(x,y)+2b_{66}\frac{\partial^3}{\partial x\,\partial y^2}u_0(x,y)+2b_{66}\frac{\partial^3}{\partial x^2\,\partial y}v_0(x,y)-4d_{66}\frac{\partial^4}{\partial x^2\,\partial y^2}w_0(x,y)+2d_{66}^S\frac{\partial^3}{\partial x^2\,\partial y}\theta_0(x,y)+2d_{66}^S\frac{\partial^3}{\partial x\,\partial y^2}\theta_0(x,y)=q(x,y) \tag{21c}$$

$$b_{11}^S\frac{\partial^2}{\partial x^2}u_0(x,y)-d_{11}^S\frac{\partial^3}{\partial x^3}w_0(x,y)+h_{11}^S\frac{\partial^2}{\partial x^2}\theta_0(x,y)+b_{12}^S\frac{\partial^2}{\partial y\,\partial x}v_0(x,y)-d_{12}^S\frac{\partial^3}{\partial y^2\,\partial x}w_0(x,y)+h_{12}^S\frac{\partial^2}{\partial y\,\partial x}\theta_0(x,y)+b_{66}^S\frac{\partial^2}{\partial y\,\partial x}u_0(x,y)+b_{66}^S\frac{\partial^2}{\partial x^2}v_0(x,y)-2d_{66}^S\frac{\partial^4}{\partial y^4}w_0(x,y)+h_{66}^S\frac{\partial^2}{\partial y\,\partial x}\theta_0(x,y)+2h_{66}\frac{\partial^2}{\partial x^2}\theta_0(x,y)+b_{66}^S\frac{\partial^2}{\partial y^2}u_0(x,y)+b_{66}^S\frac{\partial^2}{\partial y\,\partial x}v_0(x,y)-2d_{66}^S\frac{\partial^3}{\partial x\,\partial y^2}w_0(x,y)+h_{66}^S\frac{\partial^2}{\partial y^2}\theta_0(x,y)+h_{66}^S\frac{\partial^2}{\partial y\,\partial x}\theta_0(x,y)+b_{12}^S\frac{\partial^2}{\partial y\,\partial x}u_0(x,y)-d_{12}^S\frac{\partial^3}{\partial y\,\partial x^2}w_0(x,y)+h_{12}^S\frac{\partial^2}{\partial y\,\partial x}\theta_0(x,y)+b_{22}^S\frac{\partial^2}{\partial y^2}v_0(x,y)-d_{22}^S\frac{\partial^3}{\partial y^3}w_0(x,y)+h_{22}^S\frac{\partial^2}{\partial y^2}\theta_0(x,y)-a_{55}^S\theta_0(x,y)-a_{44}^S\theta_0(x,y)=0 \tag{21d}$$

5 Analytical solutions of a simply supported FGM plates

The Navier solution is used to obtain the analytical results. Displacements are presented as the product of known trigonometric coefficients and functions to satisfy the equations of motion as well as boundary conditions

$$\begin{gathered}
u_0(x,y,z)=\sum_{m=1}^{\infty}\sum_{n=1}^{\infty}u_{mn}\cos\lambda x\sin\mu y e^{iwt}\\
v_0(x,y,z)=\sum_{m=1}^{\infty}\sum_{n=1}^{\infty}\vartheta_{mn}\sin\lambda x\cos\mu y e^{iwt}\\
w_0(x,y,z)\sum_{m=1}^{\infty}\sum_{n=1}^{\infty}w_{mn}\sin\lambda x\sin\mu y e^{iwt}\\
\theta_0(x,y,z)=\sum_{m=1}^{\infty}\sum_{n=1}^{\infty}x_{mn}\cos\lambda x\sin\mu y e^{iwt}
\end{gathered} \tag{22}$$

Where $=\frac{m\pi}{a}$, $\beta=\frac{n\pi}{a}$ are the pulsations and ω is the frequency of the free vibration of the plate and $\sqrt{i}$=-1 imaginary unit. The transverse load q is also expanded in the double-Fourier sine series as:

$$q(x,y)=\sum_{m=1}^{\infty}\sum_{n=1}^{\infty}q_{mn}\sin\lambda x\sin\mu y \tag{23}$$

Substituting equations (22) and (23) into equation (21), the analytical solutions can be obtained from

$$\begin{bmatrix} k_{11} & k_{12} & k_{13}k_{14}\\ k_{21} & k_{22} & k_{23}k_{24}\\ k_{31} & k_{32} & k_{33}k_{34}\\ k_{41} & k_{42}k_{43} & k_{44}\end{bmatrix}\begin{Bmatrix}u_{mn}\\ v_{mn}\\ w_{mn}\\ x_{mn}\end{Bmatrix}=\begin{Bmatrix}0\\0\\q_{mn}\\0\end{Bmatrix} \tag{24}$$

6 Results and discussions

In this section, various numerical examples are presented and discussed to verify the accuracy of the present theory is evaluated by carrying out static analysis. The material used is the combination of two metal and ceramic materials: Al / ZrO2 and Al / Al2O3. A wide range of convergence and comparison studies are taken up in order to evaluate the accuracy of the formulation. Parametric studies are then carried out to investigate the effects of different geometric parameters on the static behaviors of FGM plates and the same are discussed in subsequent sections. The mechanical properties of these materials are grouped in Table 1.

Table 1 – Mechanical Properties of materials

Material	**E** **(*GPa*)**	ρ ***(Kg/m³)***	**Poisson's ratio** ν
Aluminum (Al*)	70	2702	0.3
Aluminum (Al)	70	2707	0.3
Zirconia (ZrO2)	151	3000	0.3
Alumina (Al2O3)	380	3800	0.3

Numerical results are presented in terms of dimensionless stresses and deflection. The various dimensionless parameters used are:

$$\begin{aligned}\bar{u}\ (z) &= \frac{100h^3E_c}{a^4q}u\left(0,\frac{b}{2},z\right)\\ \overline{\sigma_{xx}}\ (z) &= \frac{h}{aq}\sigma_{xx}\left(\frac{a}{2},\frac{b}{2},z\right)\\ \overline{\sigma_{xy}}\ (z) &= \frac{h}{aq}\sigma_{xy}(0,0,z)\\ \overline{\sigma_{xz}}\ (z) &= \frac{h}{aq}\sigma_{xz}\left(0,\frac{b}{2},z\right)\\ \bar{w}\ (z) &= \frac{10h^3E_c}{a^4q}w(\frac{ba}{2},\frac{b}{2})\end{aligned} \tag{25}$$

6.1 Application 1:

In this application, we consider a square plate FGM type A; In table 2 the results obtained from the present theory of arrow and stresses are compared for results obtained by the hyperbolic [31] and trigonometric theory [30].

Table 2 – Comparison of displacements and stresses for a square plate FGM (h/a=10; Type A)

p	Theory	$\bar{u}(-\frac{h}{4})$	$\bar{w}$	$\bar{\sigma}_{xx}(\frac{h}{3})$	$\bar{\sigma}_{xy}(-\frac{h}{3})$	$\bar{\sigma}_{xz}(\frac{h}{6})$
1	Present	0.6413	0.5889	1.5164	0.6226	0.2607
	[31]	0.6413	0.5889	1.5164	0.6226	0.2607
	[30]	0.6413	0.5890	1.4892	0.6111	0.2611
	[32]	0.6626	0.5889	1.4894	0.6110	0.2622
2	Present	0.8983	0.7572	1.4283	0.5546	0.2737
	[31]	0.8983	0.7572	1.4283	0.5546	0.2737
	[30]	0.8982	0.7573	1.3959	0.5442	0.2742

	[32]	0.9281	0.7573	1.3954	0.5441	0.2763
4	Present	1.0501	0.8814	1.2158	0.5805	0.2537
	[31]	1.0501	0.8814	1.2158	0.5805	0.2537
	[30]	1.0500	0.8816	1.1792	0.5669	0.2742
	[32]	1.0941	0.8819	1.1783	0.5667	0.2580
8	Present	1.0750	0.9846	0.9787	0.6036	0.2088
	[31]	1.0750	0.9846	0.9787	0.6036	0.2088
	[30]	1.0759	0.9746	0.9473	0.5857	0.2094
	[32]	1.1340	0.9750	0.9466	0.5856	0.2121

The variations of the arrow as well as the normal stress and the tangential stress according to the thickness are shown in Figures 3a to 3d. The values of the maximum normal stress increases with p while there appears minimal compression stresses located at inside the plate for some values of p (p≤1). The maximum value of stress tangential is located in the middle of the plate and tends to move slightly towards the upper surface compared to p.

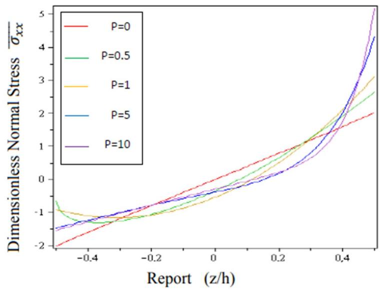

Fig. 3a –Variation of the dimensionless normal stress $\overline{\sigma_{xx}}$ respect the report (z/h) for a/h=10

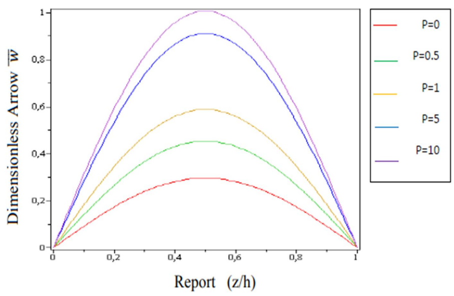

Fig. 3b –Variation of the dimensionless arrow $\overline{w}$ respect the report (z/h) for a/h=10

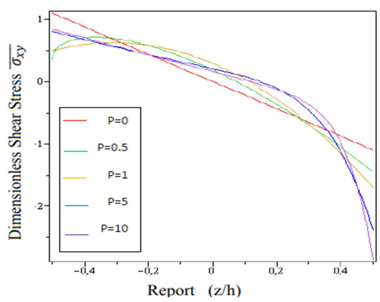

Fig. 3c –Variation of the dimensionless shear stress $\overline{\sigma_{xy}}$ respect the report (z/h) for a/h=10

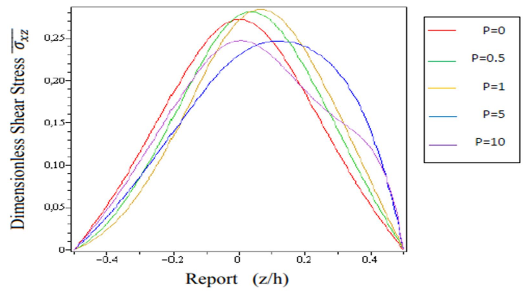

Fig. 3d–Variation of the dimensionless shear stress $\overline{\sigma_{xz}}$ respect the report (z/h) for a/h=10

6.2 Application 2:

We will study the responses of a square plate in FGM (Al / Al2O3) type B (1-2-1) under a transverse sinusoidal loading. The results obtained are compared with those obtained from the hyperbolic and trigonometric model in the table 3. The results obtained are in good agreement with those of the other models [9][10][31].

Table 3 – Comparison of displacements and stresses for a square plate FGM (h/a=10; Type B)

p	Theory	$\bar{u}(-\frac{h}{4})$	$\bar{w}$	$\bar{\sigma}_{xx}(\frac{h}{3})$	$\bar{\sigma}_{xy}(-\frac{h}{3})$	$\bar{\sigma}_{xz}(\frac{h}{6})$
1	Present	0. 3251	0.3736	1.4691	1.0024	0.2120
	[31]	0. 3251	0.3736	1.4691	1.0024	0.2120
	[30]	0. 3247	0.3744	1.4761	1.0130	0.2161
2	Present	0.6413	0.6301	1.5634	0.5526	0.2607
	[31]	0.6413	0.6301	1.5634	0.5526	0.2607
	[30]	0.7337	0.6345	1.5691	0.5447	0.2733
4	Present	1.0501	0.8156	1.2623	0.5805	0.2537
	[31]	1.0501	0.8156	1.2623	0.5805	0.2537
	[30]	1.0550	0.8331	1.2539	0.5614	0.2697
8	Present	1.0762	0.8814	1.0031	0.6086	0.2074
	[31]	1.0762	0.8814	1.0031	0.6086	0.2074
	[30]	1.0798	0.8807	0.9258	0.5758	0.21982

The variation of normal and tangential stress according to the thickness with different values of the index material p is shown in the figures 4a and 4b.

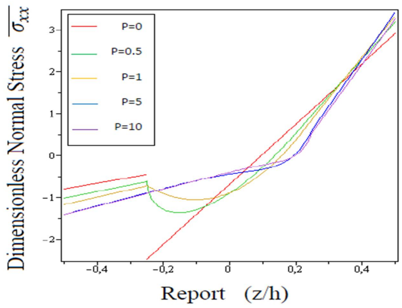

Fig. 4a –Variation of the dimensionless normal stress $\overline{\sigma_{xx}}$ respect the report (z/h) for a/h=10

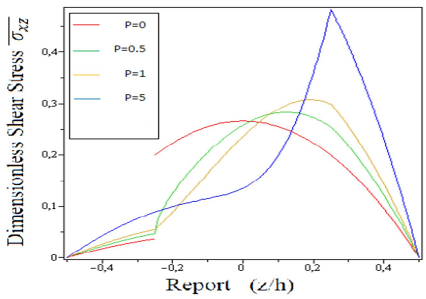

Fig. 4b –Variation of the dimensionless shear stress $\overline{\sigma_{xz}}$ respect the report (z/h) for a/h=10

6.3 Application 3:

We will study the responses of a square plate in FGM (Al / Al2O3) type C (1-2-1) under a transverse sinusoidal loading. The results obtained are compared with those obtained from the hyperbolic and trigonometric model in the table 4. The results obtained are in good agreement with those of the other models [9][10].

Table 4 – Comparison of displacements and stresses for a square plate FGM (h/a=10; Type C)

p	Theory	$\overline{w}$	$\overline{\sigma}_{xx}(\frac{h}{3})$	$\overline{\sigma}_{xz}(0)$
1	Present	0.1960	2.0157	0.2386
	Hyperbolic [10]	0.1960	2.0157	0.2386
	Trigonometric [9]	0.1959	1.9948	0.2358
2	Present	0.2709	1.3020	0.2526
	Hyperbolic [10]	0.2709	1.3020	0.2526
	Trigonometric [9]	0.2708	1.2917	0.2505
4	Present	0.3026	1.4575	0.2584
	Hyperbolic [10]	0.3026	1.4575	0.2584
	Trigonometric [9]	0.3027	1.4470	0.2564
8	Present	0.3348	1.6154	0.2651
	Hyperbolic [10]	0.3348	1.6154	0.2651

Trigonometric [9]	0.3347	1.6045	0.2632

The variation of normal and tangential stresses across the thickness is shown in Figures 5a and 5b. The maximum value of normal stress is located at level of the interfaces of the layers, against the maximum tangential stresses is located in the middle of the plate thickness.

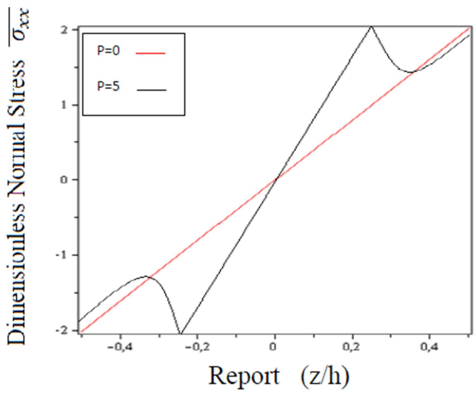

Fig. 5a –Variation of the dimensionless normal stress $\overline{\sigma_{xx}}$ respect the report (z/h) for a/h=10

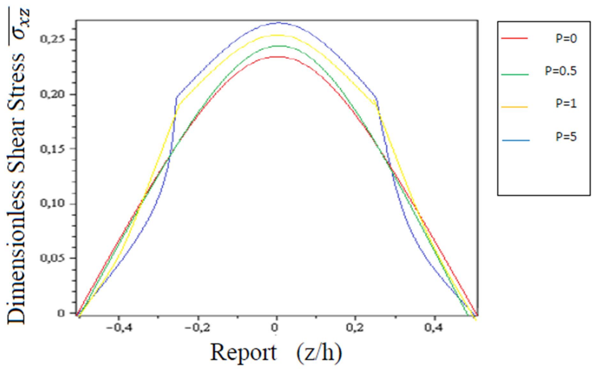

Fig. 5b –Variation of the dimensionless shear stress $\overline{\sigma_{xz}}$ respect the report (z/h) for a/h=10

7 Conclusion

A new, refined four-variable theory is proposed for static bending study of isotropic and FG sandwich plates. Three different types of FG plates are considered: FG plates, sandwich plates with FG core and sandwich plates with FG faces The results obtained by the present theory are in good agreement with the results obtained by the hyperbolic and trigonometric theories.

The values of the maximum normal stress increases with p while there appears minimal compression stresses located at inside the plate for some values of p (p≤1). The maximum value of stress tangential is located in the middle of the plate and tends to move slightly towards the upper surface compared to p.

REFERENCES

[1] Koizumi, M. “Functionally gradient materials the concept of FGM,Ceramic Transactions, vol. 34 (1993) pp. 3–10.
[2] Koizumi M. FGM activities in Japan. Compos Part B, 28 (1997) pp.1–4.
[3] Feldman, E and Aboudi, J.. Buckling analysis of functionally graded plates subjected to uniaxial loading. Compos Struct. 38 (1997) pp. 29–36.

[4] Javaher, R. and Eslami MR (2002) Buckling of functionally graded plates under in-plane compressive loading. ZAMM; http://dx.doi.org/10.1002/1521-4001(200204)82 :4%3C277: AID-ZAMM277%3E3.0.CO;2-Y.
[5] Chi SH and Chung YL Mechanical behavior of functionally graded material plates under transverse load, part I:. Analysis. Int J Solids Struct; 43 (2006) pp.3657–3674.
[6] Reissner E. The effect of transverse shear deformation on the bending of elastic plates. J. Appl. Mech. (1945) 12 pp.69–77.
[7] Mindlin RD., Influence of rotary inertia and shear on flexural motions of isotropic elastic plates. J. Appl. Mech. Vol.1 n°18 (1995) pp.31-38
[8] Menaa R, et al. Analytical solutions for static shear correction factor of functionally graded rectangular beams. Mech. Adv. Mater. Struct. 19 (2012) pp.641–652.
[9] Rashidi MM, et al., Homotopy perturbation study of nonlinear Vibration of Von Karman Rectangular Plates Comput. Struct. 106/107 (2012) pp.46–55.
[10] Zhao X, Lee YY and Liew KM. Mechanical and thermal buckling analysis of functionally graded plates. Compos. Struct. 90 (2009) pp.161–171.
[11] Moradi S and Mansouri MH. Thermal buckling analysis of shear deformable laminated orthotropic plates by differential quadrature. Steel. Compos. Struct. 12 (2012) pp.129–147.
[12] Reissner E. On transverse bending of plates, including the effect of transverse shear deformation. Int. J. Solids Struct. 11(5) (1975) pp.569-73.
[13] Reddy J.N., A general nonlinear third-order theory of functionally graded plates. Int. J. Aerosp Lightweight Struct. 1 (2011) pp.1-21.
[14] M.Touratier, (1991) “An efficient standard plate theory”, Int. J. Eng.Sci. Vol. 29,pp. 901-916.
[15] Soldatos, K., A transverse shear deformation theory for homogeneous monoclinic plates,”Acta Mech, 94 n°3 (1992) pp.195–220.
[16] Karama, M., et al. “Mechanical behavior of laminated composite beam by the new multilayered laminated composite structures model with transverse shear stress continuity,”Int. J. Solids Struct. 40 n°6 (2003) pp.1525–1546.
[17] Zenkour, A.M.. “A comprehensive analysis of functionally graded sandwich plates: Part 1-deflection and stresses”, Int. J. Solid Struct., 42 (18-19) (2005) pp.5224-5242.
[18] Li Q, Iu VP and Kou K.P. Three-dimensional vibration analysis of functionally graded material sandwich plates. J Sound Vib. 311 (2008) pp.498–515.
[19] Zenkour, A.M. and Alghamdi, N.A. “Thermoelastic bending analysis of functionally graded sandwich plates”, J. Mater. Sci., 43(8) (2008) pp.2574-2589.
[20] Addou, F.Y., et al. “Influences of porosity on dynamic response of FG plates resting on Winkler/Pasternak/Kerr foundation using quasi 3D HSDT, Comput. Concrete, Int. J., 24(4) (2019) pp.347-367.
[21] Boukhlif, Z., et al. “A simple quasi-3D HSDT for the dynamics analysis of FG thick plate on elastic foundation”, Steel Compos. Struct., Int. J., 31(5) (2019) pp.503-516.
[22] Boulefrakh, L., et al. “The effect of parameters of visco-Pasternak foundation on the bending and vibration properties of a thick FG plate”,Geomech. Eng., Int. J., 18(2) (2019) pp.161-178.
[23] Boutaleb, S.,et al. “Dynamic Analysis of nanosize FG rectangular plates based on simple nonlocal quasi 3D HSDT”, Adv. Nano Res., Int. J., 7(3) (2019) pp.189-206.
[24] Khiloun, M., et al. “Analytical modeling of bending and vibration of thick advanced composite plates using a four-variable quasi 3D HSDT”, Eng. Comput. (2019).
[25] Mahmoudi, A. et al. “A refined quasi-3D shear deformation theory for thermo-mechanical behavior of functionally graded sandwich plates on elastic foundations”, J. Sandw. Struct. Mater., 21(6) (2019) pp.1906-1926.
[26] Zaoui, F.Z., Ouinas, D. and Tounsi, A. “New 2D and quasi-3D shear deformation theories for free vibration of functionally graded plates on elastic foundations”, Compos. Part B, 159 (2019) pp.231-247.
[27] Zarga, D., et al., (2019), “Thermomechanical bending study for functionally graded sandwich plates using a simple quasi-3D shear deformation theory”,Steel Compos. Struct., Int. J., 32(3), 389-410. https://doi.org/10.12989/scs.2019.32.3.389
[28] Mahi A, Adda BEA and Tounsi A. A new hyperbolic shear deformation theory for bending and free vibration analysis of isotropic, functionally graded, sandwich and laminated composite plates. Appl. Math. Model. 39 (2015) pp.2489–2508.

[29] Merdaci, S. Analytical solution for free vibration analysis of plates functionally graded FGP with porosities. Recueil de Mécanique , vol.4 n°2 (2019)pp.397-408.

[30] Van-Hau Nguyen, et al. A new inverse trigonometric shear deformation theory for isotropic and functionally graded sandwich plates. Composites: Part B 66 (2014) pp.233-246.

[31] Reddy JN.. Analysis of functionally graded plates. Int. J. Numer. Methods Eng. 47/663-84 (2000).

[32] Zenkour AM.. Generalized shear deformation theory for bending analysis of functionally graded materials. Appl. Math. Model, 30(2006) pp.67-84.